

The cooling effect on structural, electrical, and optical properties of epitaxial a-plane ZnO:Al on r-plane sapphire grown by pulsed laser deposition

Chun-Yen Peng, Yuan-An Liu, Wei-Lin Wang, Jr-Sheng Tian, and Li Chang

Citation: [Applied Physics Letters](#) **101**, 151907 (2012); doi: 10.1063/1.4759032

View online: <http://dx.doi.org/10.1063/1.4759032>

View Table of Contents: <http://scitation.aip.org/content/aip/journal/apl/101/15?ver=pdfcov>

Published by the [AIP Publishing](#)

Articles you may be interested in

[Structure and optical properties of a-plane ZnO/Zn_{0.9}Mg_{0.1}O multiple quantum wells grown on r-plane sapphire substrates by pulsed laser deposition](#)

[J. Appl. Phys.](#) **112**, 103519 (2012); 10.1063/1.4767462

[Magnetotransport properties of high quality Co:ZnO and Mn:ZnO single crystal pulsed laser deposition films: Pitfalls associated with magnetotransport on high resistivity materials](#)

[Rev. Sci. Instrum.](#) **81**, 063902 (2010); 10.1063/1.3436648

[A study of H and D doped ZnO epitaxial films grown by pulsed laser deposition](#)

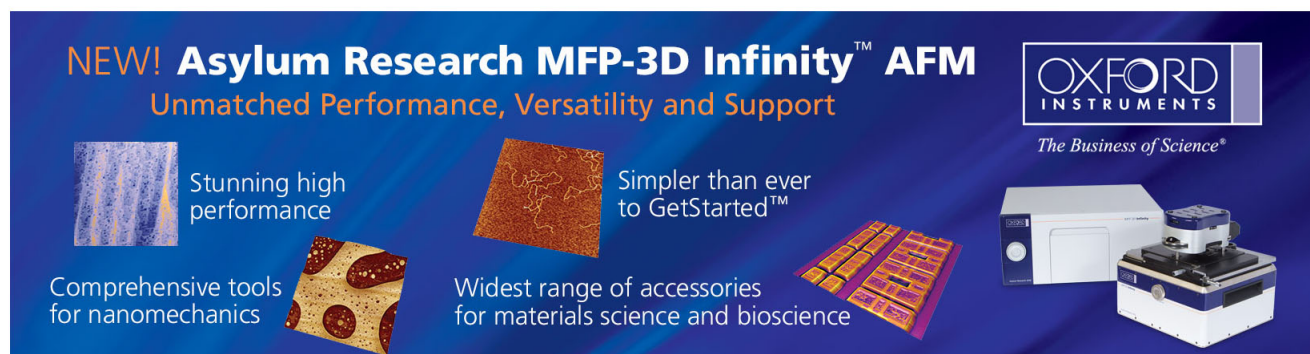
[J. Appl. Phys.](#) **104**, 053711 (2008); 10.1063/1.2975219

[Low resistivity polycrystalline ZnO:Al thin films prepared by pulsed laser deposition](#)

[J. Vac. Sci. Technol. A](#) **22**, 1757 (2004); 10.1116/1.1763903

[Optical properties of epitaxially grown zinc oxide films on sapphire by pulsed laser deposition](#)

[J. Appl. Phys.](#) **86**, 408 (1999); 10.1063/1.370744



NEW! Asylum Research MFP-3D Infinity™ AFM
Unmatched Performance, Versatility and Support

OXFORD INSTRUMENTS
The Business of Science®

Stunning high performance
Simpler than ever to GetStarted™
Comprehensive tools for nanomechanics
Widest range of accessories for materials science and bioscience

The advertisement features several images: a blue textured surface, a brown textured surface, a grid of colorful rectangular samples, and the Asylum Research MFP-3D Infinity AFM instrument.

The cooling effect on structural, electrical, and optical properties of epitaxial *a*-plane ZnO:Al on *r*-plane sapphire grown by pulsed laser deposition

Chun-Yen Peng, Yuan-An Liu, Wei-Lin Wang, Jr-Sheng Tian, and Li Chang^{a)}

Department of Materials Science and Engineering, National Chiao Tung University, 30010 Hsinchu, Taiwan

(Received 13 July 2012; accepted 1 October 2012; published online 11 October 2012)

Here, the unambiguous effect of cooling rate on structural, electrical, and optical properties of *a*-plane ZnO:Al on *r*-plane sapphire grown by pulsed laser deposition at 700 °C is reported. A high cooling rate (~ 100 °C/min) can result in stripe morphology along *m*-direction and significant deformation on the epitaxial films of *a*-plane ZnO:Al with deteriorated crystallinity and significantly lowered resistivity. Also, photoluminescence spectra exhibit high intensities of excess violet and green emissions with low intensity of near band edge luminescence. Comparison with pure *a*-plane ZnO films is also presented. © 2012 American Institute of Physics.

[<http://dx.doi.org/10.1063/1.4759032>]

As a wide direct bandgap wurtzite semiconductor, zinc oxide (ZnO) is an attractive material for potential applications in light emitting devices, transparent thin-film transistors, and transparent electrodes. Especially, it exhibits an intense near-band-edge excitonic emission at room temperature due to its large exciton binding energy (~ 60 meV), and low electrical resistivity with high transparency can be achieved by doping with Al, Ga, and In. These advantages of ZnO-based materials have attracted much attention in the last few years.

Because of the low cost, abundant resource availability and low electrical resistivity compared with other IIIA impurities, Al-doped ZnO (AZO) is a potential transparent conducting oxide (TCO) to replace for indium tin oxide.¹ Though deposition of polycrystalline AZO as TCO has been intensively studied for practical applications, fundamental understanding is still lacking. Epitaxial ZnO films doped with Al (ZnO:Al) may be beneficial for studying the properties of TCO due to better crystallinity.

Recently, the growth of nonpolar epitaxial films has attracted a lot of interest as nonpolar ZnO can have better light emitting performance without the quantum confined Stark effect often observed in *c*-plane ZnO.²⁻⁵ *R*-plane sapphire is a commonly used substrate for growth of *a*-plane ZnO films. However, there are large anisotropic structural properties along two in-plane directions between nonpolar ZnO and substrate. For example, the lattice mismatch between ZnO [0001] and sapphire $[\bar{1}01\bar{1}]$ is 1.5% and the thermal mismatch is -40.8% , while the lattice mismatch between ZnO $[\bar{1}100]$ and sapphire $[1\bar{2}10]$ is 18.3% and the thermal mismatch is 7%.⁶⁻⁸ Such large anisotropic structural properties may strongly affect the crystallinity of epitaxial film.

For actual light-emitting devices, a good and stable *n*-type layer of *a*-plane ZnO is required as well. Among various doped ZnO, ZnO:Al is a promising *n*-type candidate.

Only a few reports have shown growth of epitaxial *a*-plane ZnO:Al on *r*-sapphire with properties,⁹⁻¹¹ though the effects of large anisotropic lattice mismatch between ZnO and sapphire on structural properties have been reported by many studies.¹²⁻¹⁶ In this paper, the effect of cooling rate on the crystal, electrical, and optical properties for epitaxial *a*-plane ZnO:Al on *r*-plane sapphire is reported, which are significantly different from those of ZnO deposited under identical conditions.

ZnO:Al epitaxial films were deposited by pulsed laser deposition (PLD) in a home-made system and a Pascal laser molecular beam epitaxy (laser-MBE) system. For dedicated cooling experiments, the film deposition was carried out in the Pascal laser-MBE system, which was equipped with a fiber optic pyrometer, a proportional integral derivative controller, and an infrared diode laser on the substrate coupled with a 10×10 mm² back plate to provide accurate closed-loop temperature control for heating and cooling. The substrates of *r*-plane sapphire were in a size of 8×8 mm². Before deposition, the substrate was heated to 850 °C for thermal cleaning in vacuum of about 10^{-6} torr for 30 min in the chamber. The growth conditions were the substrate temperature at 700 °C with 10 mtorr oxygen partial pressure. Ablation was done by applying a pulsed KrF excimer laser (~ 3 J/cm², 5 Hz) on a sintered target fabricated from the mixture of 99.0 wt. % ZnO and 1.0 wt. % Al₂O₃ powders with 99.9% purity. For controlled cooling experiments, 200 nm thick films were grown, followed by direct cooling with different rate in oxygen ambient of 10 mTorr. For comparison, pure ZnO films were also grown under the same condition with controlled cooling. To evaluate crystallinities, x-ray diffraction (XRD) with x-ray rocking curves (XRCs) and reciprocal space maps (RSM) were performed in a PANalytical X'Pert Pro (MRD) high-resolution x-ray diffraction system employing a Ge (220) monochromator and Ge (220) channel cut analyzer. Surface morphologies of the deposited films were examined in a JEOL JSM-6700F field emission scanning electron microscope (SEM) and a Veeco Dimension 5000 atomic force microscope (AFM) operated in tapping mode. The electrical properties were determined by using the van der Pauw method with a magnetic field of

^{a)} Author to whom correspondence should be addressed. Electronic mail: lichang@cc.nctu.edu.tw. Tel.: 886-3-5731615. FAX: 886-3-5724727. Department of Materials Science and Engineering, National Chiao Tung University, 1001, Tahsueh Road, Hsinchu 300, Taiwan.

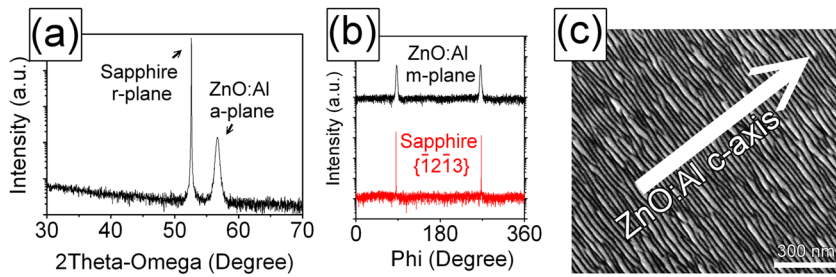


FIG. 1. (a) X-ray $2\theta/\theta$ diffraction pattern, (b) phi-scan patterns, and (c) SEM image of a -plane ZnO:Al film on sapphire.

0.3 T at room temperature (ACCENT HL5500 Hall measurement system). The photoluminescence (PL) spectra were acquired at 12 K by using a 325 nm Hd-Cd laser with power of about 15 mW as the excitation light source.

A typical x-ray $2\theta/\theta$ diffraction pattern of ZnO:Al films on r -plane sapphire is shown in Fig. 1(a), illustrating that only the peaks of sapphire r -plane and ZnO:Al a -plane can be seen at 52.55° and 56.68° without other peaks. Also, the phi-scan pattern in Fig. 1(b) shows the positions of ZnO $\{1\bar{1}00\}$ peaks in coincidence with sapphire $\{12\bar{1}3\}$ and $(2\bar{1}13)$ with spacing angle of 180° , indicating that the epitaxial relationship between a -plane ZnO:Al and sapphire is $(11\bar{2}0)_{\text{ZnO:Al}} // (1102)_{\text{sapphire}}$ and $[1\bar{1}00]_{\text{ZnO}} // [\bar{1}2\bar{1}0]_{\text{sapphire}}$ as ZnO grown on r -plane sapphire. Figure 1(c) shows a typical SEM image of the ~ 200 nm thick ZnO:Al epitaxial films. At first sight, it looks like a stripy morphology commonly observed on a -plane ZnO film. Interestingly, after determination of the in-plane directions, the stripes shown in Fig. 1(c) are actually normal to its c -direction different from stripes parallel to its c -direction usually seen on a -plane ZnO.¹² The average width of these stripes is about 20–30 nm. The m -direction stripe characteristics have been observed on a -plane GaN by Craven *et al.*¹⁷ Also, it is known that the stress may play a significant role on surface morphology due to strain relaxation of a film,^{18–21} which can arise from the large thermal mismatch along $[0001]_{\text{ZnO}}$ direction with r -plane sapphire. Hence, the features of stripe-like morphology with grooves observed in the ZnO:Al films might be related to its growth evolution and thermal stress. To verify the effect of thermal stress on such stripe-like morphology of a -plane ZnO:Al epitaxial film, we therefore carried out controlled cooling experiments after film growth of ZnO

and ZnO:Al under the same deposition conditions for comparison.

Figure 2 shows AFM surface morphologies of ZnO and ZnO:Al epitaxial films with 30 and $100^\circ\text{C}/\text{min}$ cooling rates. For pure ZnO grown on r -plane sapphire with 30 and $100^\circ\text{C}/\text{min}$ cooling rates, smooth surfaces with stripes along $[0001]_{\text{ZnO}}$ are observed in Figs. 2(a) and 2(b). Generally, both cooling rates do not have significant effects on surface roughness and morphology of the ZnO films. However, there are a few grooves along $[\bar{1}100]_{\text{ZnO}}$, which can be clearly seen in three dimensional perspective view as shown in Fig. 2(c) for a -plane ZnO epitaxial film with $100^\circ\text{C}/\text{min}$ cooling rate. Such grooves have ~ 0.5 nm depth with ~ 20 – 80 nm spacing. In contrast, relatively rougher surfaces are observed on ZnO:Al epitaxial films as shown in Figs. 2(d) and 2(e). However, large and coarse stripy islands elongated along $[0001]_{\text{ZnO}}$ can be recognized in Fig. 2(e), which actually consist of many fine stripes with grooves along $[\bar{1}100]_{\text{ZnO}}$ as shown in Figs. 2(e) and 2(f) similar to the above SEM observation. For the $30^\circ\text{C}/\text{min}$ cooled ZnO:Al, while the island-like morphology is clearly seen in Fig. 2(d), the fine stripes with shorter length can also be observed along $[\bar{1}100]_{\text{ZnO}}$. It is noticed that there exist a higher density of fine stripes with grooves on the ZnO:Al film with higher cooling rate. These fine stripes width along ZnO c -direction are about 20–30 nm width with 0.5–1 nm deep grooves for both ZnO:Al films with different cooling rate.

In addition to the appearance of a high density of fine stripes with grooves along m -direction with high cooling rate, the cooling effect on crystallinities has been also investigated with XRCs and RSMs. Figures 3(a) and 3(b) show XRCs of ZnO epitaxial films with 30 and $100^\circ\text{C}/\text{min}$

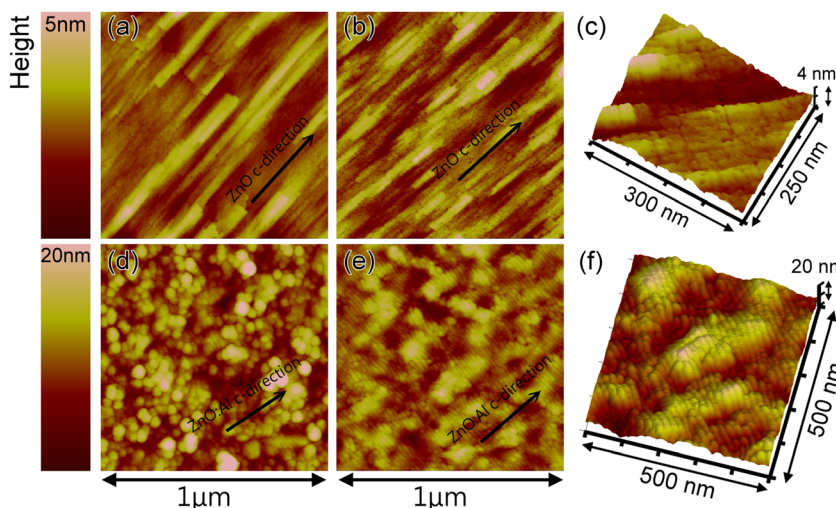


FIG. 2. AFM images of (a)–(c) ZnO and (d)–(f) ZnO:Al films with (a) and (e) $30^\circ\text{C}/\text{min}$ and (b), (c), (e), and (f) $100^\circ\text{C}/\text{min}$ cooling rates.

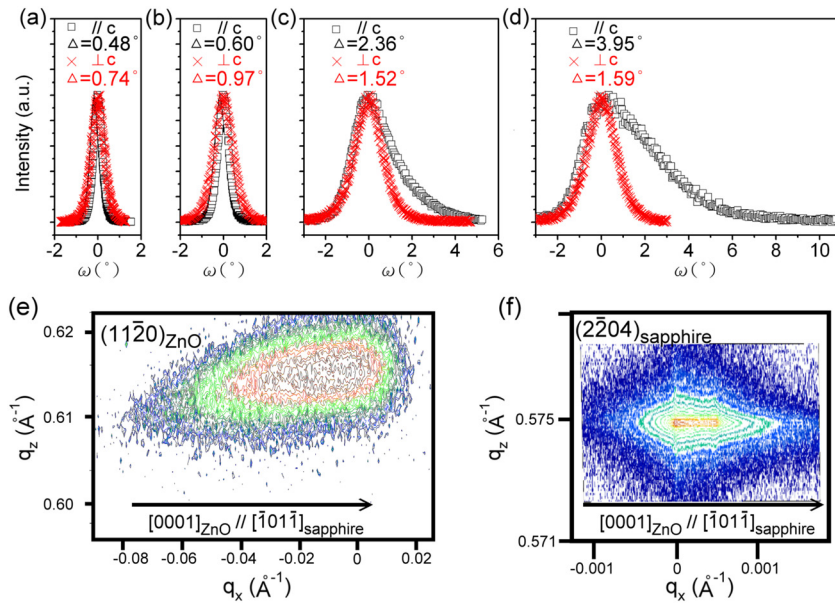


FIG. 3. XRCs of (a) and (b) ZnO and (c) and (d) ZnO:Al films with (a) and (c) 30°C/min and (b) and (d) 100°C/min cooling rates. (e) and (f) $(11\bar{2}0)_{\text{ZnO:Al}}$ and $(2\bar{2}04)_{\text{sapphire}}$ RSMs for the ZnO:Al film on sapphire with 100°C/min cooling rate.

cooling, respectively. The full width at half maximum (FWHM) of XRC $//c_{\text{ZnO}}$ is narrower than that of $\perp c_{\text{ZnO}}$ for both pure-ZnO films as reported in the literatures due to large lattice mismatch present in ZnO m -direction makes c -mosaic greater than m -mosaic for a -plane ZnO grown on r -plane sapphire.²² Also, it is illustrated that the higher cooling rate can result in degradation of crystallinity as the FWHMs of both XRCs $//c$ and $\perp c$ are broadened from 0.48° to 0.60° and 0.74° to 0.97°, respectively. However, crystallinities of ZnO:Al epitaxial films grown on r -plane sapphire along $//c_{\text{ZnO}}$ and $\perp c_{\text{ZnO}}$ exhibit different characteristics as XRCs in Figs. 3(c) and 3(d) show the larger FWHM in $//c$ than $\perp c$. The FWHMs of XRCs $\perp c$ for both films are in the range of 1.5°–1.6°, while the FWHM of XRC $//c$ is 2.36° for 30°C/min and 3.96° for 100°C/min. Also, the broad XRCs $//c$ for ZnO:Al exhibit extended asymmetric distribution, which has been further examined with RSMs as shown in Figs. 3(e) and 3(f) for the reflections of $(11\bar{2}0)_{\text{ZnO:Al}}$ and $(2\bar{2}04)_{\text{sapphire}}$ from the ZnO:Al film with 100°C/min cooling rate. A long extended asymmetrical tail is seen in Fig. 3(e) for $(11\bar{2}0)_{\text{ZnO:Al}}$ consistent with the asymmetric distribution observed in XRC. Also, an asymmetrical intensity distribution in the opposite direction can be seen in Fig. 3(f) for $(2\bar{2}04)_{\text{sapphire}}$. Hence, it may indicate that both the ZnO:Al epitaxial film and sapphire substrate are tilted around the rotation axis of $[11\bar{2}0]_{\text{sapphire}}$ towards opposite directions away from each other. As such opposite tilting of sapphire reflection away from ZnO:Al one, they might have compensated with bending strains or deformation from each other,

probably due to thermal stresses caused by cooling. For the pure ZnO films, however, no such phenomena can be observed in RSMs (not shown). Therefore, it is reasonably believed that Al dopants play a critical role on the deformation in the films due to the cooling effect. Further investigation may need to understand the exact role of Al dopants in the a -plane ZnO:Al film with cooling.

Hall measurements for ZnO:Al epitaxial films with 30 and 100°C/min cooling show that the carrier concentrations are 3.5×10^{20} and $6.7 \times 10^{20} \text{ cm}^{-3}$, respectively. Interestingly, even though the cooling rate has a significant effect on the crystallinities, a lowered resistivity of $6.37 \times 10^{-4} \Omega\text{-cm}$ has been obtained for the 100°C/min cooled ZnO:Al film than $1.62 \times 10^{-3} \Omega\text{-cm}$ for the 30°C/min cooled one. As the electron concentration may be compensated with oxygen,^{9,23} higher cooling rate with oxygen ambient could reduce the exposure time to oxygen during the cooling process. As a result, the lower resistivity with higher carrier concentration can be obtained from the sample with higher cooling rate. For the pure ZnO films, the cooling rate does not have a significant effect on the electrical properties, which show the resistivities in the order of $10^{-2} \Omega\text{-cm}$ with carrier concentrations of 10^{18} cm^{-3} . In comparison with ZnO, ZnO:Al can have better electrically conducting properties with worse crystallinity.

Figure 4 shows low-temperature PL spectra of ZnO and ZnO:Al. In Fig. 4(a), it is observed that luminescences of the pure ZnO epitaxial films are simply dominated by near band edge emissions with deep level emissions being hardly seen.

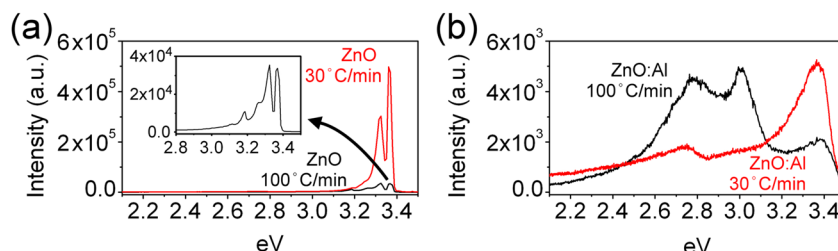


FIG. 4. Low temperature PL spectra of (a) ZnO and (b) ZnO:Al films with 30°C/min (black curve) and 100°C/min cooling rates (red curve). The inset in (a) is an enlarged spectrum of 100°C/min cooled ZnO showing the near band edge region.

For near band edge emissions in both 30 and 100 °C/min cooled ZnO films, typical bound exciton recombination (D^0 , X) appears at ~ 3.35 eV (~ 20 meV FWHM) and defect-related emission (A^0 , X) at ~ 3.31 eV (~ 30 meV FWHM).^{24–26} Also, it is noticed that the difference in cooling rate makes significant variation on PL intensity. The intensity of (D^0 , X) emission for 30 °C/min cooled ZnO is one order of magnitude higher than that of 100 °C/min one under the same experimental condition for PL measurements. Also, the luminescence intensity ratio of (D^0 , X):(A^0 , X) is decreased from 2:1 (30 °C/min) to 1:1 (100 °C/min). For the ZnO:Al epitaxial films, the variation of PL characteristics with cooling rate is significantly different from ZnO films. Not only broader near band edge emissions appear at different positions with dissimilar intensity but also deep level emissions exhibit varied distribution as shown in Fig. 4(b). It shows the near band edge emission peak at ~ 3.37 eV with 186 meV FWHM and typical V_O -related deep level green emission²⁷ at ~ 2.74 eV for the 30 °C/min cooled ZnO:Al epitaxial film. With 100 °C/min cooling rate, the ZnO:Al epitaxial film shows about two and half times lower intensity for the near band edge emission peak compared with the 30 °C/min sample. Also, deep level green emission at ~ 2.77 eV and excess Zn_i related deep level violet emission²⁷ at ~ 3.01 eV are observed in Fig. 4(d) for the 100 °C/min cooled ZnO:Al epitaxial film. It is known that higher carrier concentration may result in broader near band edge emission due to impurity band broadening.^{28,29} However, such broader near band edge emissions are not observed in the *c*-plane ZnO:Al epitaxial film, which has $1.7 \times 10^{20} \text{ cm}^{-3}$ carrier concentration.³⁰ Also, the V_O -related deep level and excess Zn_i related emissions are only appeared in our ZnO:Al epitaxial films with intensity increasing with cooling rate. Accordingly, the broader near band edge emissions with excess deep level emissions observed in the *a*-plane ZnO:Al epitaxial films may be resulted from Al-related defects in ZnO, which are generated from cooling.

In summary, crystallinity deterioration has been observed in Al-doped *a*-plane ZnO epitaxial films grown on *r*-plane sapphires with cooling rate of 30 and 100 °C/min in comparison with ZnO. Asymmetrical deformation of the *a*-plane ZnO:Al films in *c*-direction and fine stripes along $[\bar{1}100]_{\text{ZnO:Al}}$ are only observed in Al-doped ZnO films with fast cooling rate. Also, the ZnO:Al film with higher cooling rate shows lower resistivity but with worse crystallinity. Finally, the difference in cooling rate may result in lower luminescence intensity and significant change on photoluminescence properties of *a*-plane ZnO:Al films.

The authors gratefully acknowledge the National Science Council (Taiwan, ROC) for supporting this work (NSC Contract No. NSC98-2221-E-009-042-MY3).

- ¹T. Minami, *Semicond. Sci. Technol.* **20**, S35 (2005).
- ²T. Makino, A. Ohtomo, C. H. Chia, Y. Segawa, H. Koinuma, and M. Kawasaki, *Physica E* **21**, 671 (2004).
- ³T. Makino, Y. Segawa, M. Kawasaki, and H. Koinuma, *Semicond. Sci. Technol.* **20**, S78 (2005).
- ⁴M. Brandt, M. Lange, M. Stölzel, A. Müller, G. Benndorf, J. Zippel, J. Lenzner, M. Lorenz, and M. Grundman, *Appl. Phys. Lett.* **97**, 052101 (2010).
- ⁵M. Lange, C. P. Dietrich, K. Brachwitz, M. Stölzel, M. Lorenz, and M. Grundmann, *Phys. Status Solidi RRL* **6**, 31 (2012).
- ⁶W. M. Yim and R. J. Paff, *J. Appl. Phys.* **45**, 1456 (1974).
- ⁷CINDAS LLC, Thermophysical Properties of Matter Database 7 (2011). <https://cindasdata.com/Applications/TPMD/>.
- ⁸H. Sawada, R. Wang, and A. W. Sleight, *J. Solid State Chem.* **122**, 148 (1996).
- ⁹V. Srikant, V. Sergio, and D. R. Clarke, *J. Am. Ceram. Soc.* **78**, 1931 (1995).
- ¹⁰P. Kuppasami, G. Vollweiler, D. Rafaja, and K. Ellmer, *Appl. Phys. A* **80**, 183 (2005).
- ¹¹M. Kumar, R. M. Mehra, and S.-Y. Choi, *Curr. Appl. Phys.* **9**, 737 (2009).
- ¹²H. Wang, C. Chen, Z. Gong, J. Zhang, M. Gaeovski, M. Su, J. Yang, and M. Asif Hkan, *Appl. Phys. Lett.* **84**, 499 (2004).
- ¹³J.-M. Chauveau, P. Vennéguès, M. Lüigt, C. Deparis, J. Zuniga-Perez, and C. Morhain, *J. Appl. Phys.* **104**, 073535 (2008).
- ¹⁴G. Saraf, Y. Luc, and T. Siegrist, *Appl. Phys. Lett.* **93**, 041903 (2008).
- ¹⁵C. C. Kuo, W.-R. Liu, W. F. Hsieh, C.-H. Hsu, H. C. Hsu, and L. C. Chen, *Appl. Phys. Lett.* **95**, 011905 (2009).
- ¹⁶P. Pant, J. D. Buadi, and J. Narayan, *Acta Mater.* **58**, 1097 (2010).
- ¹⁷M. D. Craven, F. Wu, A. Chakraborty, B. Imer, U. K. Mishra, S. P. Den-Barrs, and J. S. Speck, *Appl. Phys. Lett.* **84**, 1281 (2004).
- ¹⁸C. W. Snyder, B. G. Orr, D. Kessler, and L. M. Sander, *Phys. Rev. Lett.* **66**, 3032 (1991).
- ¹⁹S. J. Hearne, J. Han, S. R. Lee, J. A. Floro, D. M. Follstaedt, E. Chason, and I. S. T. Tsong, *Appl. Phys. Lett.* **76**, 1534 (2000).
- ²⁰K. Ito, K. Hiramatsu, H. Amano, and I. Akasaki, *J. Cryst. Growth* **104**, 533 (1990).
- ²¹E. C. Young, A. E. Romanov, C. S. Gallinat, A. Hirai, G. E. Beltz, and J. S. Speck, *Appl. Phys. Lett.* **96**, 041913 (2010).
- ²²S. K. Han, S. K. Hong, J. W. Lee, J. Y. Lee, J. H. Song, Y. S. Nam, S. K. Chang, T. Minegishi, and T. Yao, *J. Cryst. Growth* **309**, 121 (2007).
- ²³S. Lany and A. Zunger, *Phys. Rev. Lett.* **98**, 045501 (2007).
- ²⁴J.-M. Chauveau, C. Morhain, B. Lo, B. Vinter, P. Vennéguès, M. Lüigt, D. Buell, M. Tesseire-Doninelli, and G. Neu, *Appl. Phys. A* **88**, 65 (2007).
- ²⁵J. Fallert, R. Hauschild, F. Stelzl, A. Urban, M. Wissinger, H. Zhou, C. Klingshirn, and H. Kalt, *J. Appl. Phys.* **101**, 073506 (2007).
- ²⁶M. Schirra, R. Schneider, A. Reiser, G. M. Prinz, M. Feneberg, J. Biskupek, U. Kaiser, C. E. Krill, K. Thonke, and R. Sauer, *Phys. Rev. B* **77**, 125215 (2008).
- ²⁷C. H. Ahn, Y. Y. Kim, D. C. Kim, S. K. Mohanta, and H. K. Cho, *J. Appl. Phys.* **105**, 013502 (2009).
- ²⁸T. N. Morgan, *Phys. Rev.* **139**, A343 (1965).
- ²⁹E. Iliopoulos, D. Doppalapudi, H. M. Ng, and T. D. Moustakas, *Appl. Phys. Lett.* **73**, 375 (1998).
- ³⁰J. H. Noh, I. S. Cho, S. Lee, C. M. Cho, H. S. Han, J. S. An, C. H. Kwak, J. Y. Kim, H. S. Jung, J. K. Lee, and K. S. Hong, *Phys. Status Solidi A* **206**, 2133 (2009).